Revista Brasileira de Farmacognosia 28 (2018) 433–443

Brazilian Journal of Pharmacognosy
REVISTA BRASILEIRA DE FARMACOGNOSIA
www.elsevier.com/locate/bjp

Original Article

Physicochemical, biological and release studies of chitosan membranes incorporated with *Euphorbia umbellata* fraction

Bruna M. Lemes[a], Andressa Novatski[b], Priscileila C. Ferrari[a], Bruno R. Minozzo[a], Aline da S. Justo[a], Victor E.K. Petry[a], José C.R. Vellosa[c], Simone do R.F. Sabino[b], Jaqueline V. Gunha[b], Luís A. Esmerino[c], Flávio L. Beltrame[a,*]

[a] *Departamento de Ciências Farmacêuticas, Universidade Estadual de Ponta Grossa, Ponta Grossa, PR, Brazil*
[b] *Departamento de Física, Universidade Estadual de Ponta Grossa, Ponta Grossa, PR, Brazil*
[c] *Departamento de Análises Clínicas e Toxicológicas, Universidade Estadual de Ponta Grossa, Ponta Grossa, PR, Brazil*

ARTICLE INFO

Article history:
Received 17 October 2017
Accepted 1 May 2018
Available online 24 May 2018

Keywords:
Bark methanolic fraction
Chemical interactions
Medicine
Phenolic compounds
Physicochemical characterization
Release profile

ABSTRACT

Formulations containing chitosan incorporated with methanolic fraction of *Euphorbia umbellata* (Pax) Bruyns, Euphorbiaceae, were studied aiming future applications of this new material as medicine. In order to investigate potential interactions between chitosan and the methanolic fraction (10, 50 and 100% in relation to the amount of chitosan) physicochemical characterization was performed by scanning electron microscopy, density, differential scanning calorimetry, thermogravimetry, X-ray diffraction, Fourier-transform infrared spectroscopy and colorimetry techniques. The phenolic compounds released from the chitosan membranes were evaluated using the Folin-Ciocalteau quantification method; antioxidant and antimicrobial activity were also studied. Increasing amounts of the methanolic fraction added to polymeric matrix produced different numbers of pores on the surface of the membranes, changes in the calorimetric, spectroscopic and crystalline properties as well as color changes, when compared to the inert membrane. These changes can be attributed to chemical interactions that occurred between the structure of the chitosan and the phenolic compounds present in the studied fraction. The matrix samples incorporated with 50 and 100% of the methanolic fraction presented different release profiles of phenolic compounds from the membranes (controlled manner) and promoted antioxidant and antimicrobial activity.

Introduction

Chitosan is a biodegradable, biocompatible, non-toxic polymer, with a cationic and hydrophilic character. It is composed of the linear monomer units (1,4)-2-acetamido-2-deoxy-D-glucopyranose, and 2-amino-2-deoxy-D-glucopyranose (Dias et al., 2013). Its solubility in water occurs in acidic medium due to the protonation of the amino group in the second carbon atom of glucosamine (Senel and Mcclure, 2004). It is characterized by containing three different functional groups in its structure: amine, acetamide and hydroxyl. The amine grouping has a cationic character that favors its ability to interact or react with different compounds (Abdel-Rahman et al., 2016).

Chitosan has gained growing interest recently because it is a promising natural substance that can be used in the biomedical field and in the chemical, pharmaceutical and food industries (Abdel-Rahman et al., 2016). Due to the great capacity of accelerating wound healing, chitosan has been widely used for the topical treatment of wounds (Coqueiro and Di Piero, 2011; Abdel-Rahman et al., 2016).

Chitosan is capable of stimulating cellular proliferation and migration; providing proteins for healing; strengthening the formation of tissue; acting as a barrier against microorganisms; minimizing skin deformation; stimulating natural blood coagulation; absorbing fluids (exudates); guiding the reorganization of the cellular histoarchitecture of wounds; and blocking nerve endings, thereby reducing pain (Freitas et al., 2011; Prichystalová et al., 2014; Benhabiles et al., 2012).

The polymeric characteristic of chitosan allows it to generate porous structures that can be used in the formulations of

* Corresponding author.
E-mail: flaviobeltra@uepg.br (F.L. Beltrame).

https://doi.org/10.1016/j.bjp.2018.05.001

dressings and controlled-release drug products such as membranes, nanoparticles and microspheres (Denkbas and Ottenbrite, 2006; Dias et al., 2013). The membranes are prepared by evaporating a chitosan dispersion that is dispersed in acetic acid on a support, which results in the formation of a flexible and resistant film (Leceta et al., 2013; Wang et al., 2013). Chitosan membranes associated with other polymers and incorporated with different substances such as antibiotics, have beneficial effects in the control of infection and promotion of wound healing (Bernkop-Schnürch and Dünnhaupt, 2012).

Phenolic compounds are a group of substances with different degrees of chemical complexity, which have the ability to neutralize reactive oxygen species (ROS) and have antioxidant activity that is often related to a wide range of biological effects (Quideau et al., 2011). Recent studies have reported a strong correlation between the amount of phenolic compounds present in plant extracts and their biological activities (Timmers et al., 2015; Nađpal et al., 2016). Some studies have evaluated the addition of plant extracts that are rich in phenolic compounds to chitosan membranes in order to explore the biological benefits of this mixture (Martel-Estrada et al., 2015).

Euphorbia umbellata (Pax) Bruyns, (synonymous: *Synadenium grantii* Hook. f., *Synadenium umbellatum* Pax, *Synadenium umbellatum* var. *puberulum*), is popularly known in Brazil as *janaúba* and *leitosinha* and has been used in folk medicine for its anti-inflammatory, anti-ulcer, homeostatic and angiogenic properties. Previous ethnopharmacological studies have demonstrated the antioxidant and anti-inflammatory activities of stem bark extracts and have related these effects to the presence of phenolic compounds. Additionally, data shown that crude bark hydroalcoholic extract of *E. umbellata* (CBE) and its methanolic fraction (MF) did not cause gastric lesions (300 mg/kg/day, oral administration, 5 days (CBE), or 200 mg/kg, oral administration, single dose (MF)) or renal and hepatic function changes (100 mg/kg/day, oral administration, 5 days) revealed by serum biomarkers (urea, creatinine, glutamic oxaloacetic transaminase, glutamic pyruvic transaminase). Furthermore, no changes in animal behavior (food or water intake), weight or organs (macroscopic evaluation of the liver, spleen, kidneys) were observed with the doses evaluated (Munhoz et al., 2014; Minozzo et al., 2016).

Thus, this study purposes the development of chitosan membranes incorporated with the methanolic fraction of *E. umbellata* extract as well as their physicochemical characterization and release profile, antioxidant potential and microbiological activity evaluation aiming future applications of this new formulation as topical treatment of wounds.

Materials and methods

Botanical identification of plant material and obtaining the extract and fractions

The plant material (*Euphorbia umbellata* (Pax) Bruyns, Euphorbiaceae) was collected in the region of Ponta Grossa (Brazil), altitude: 975 meters, latitude: 25°05′38″ S, longitude: 50°09′30″ W. A voucher specimen was prepared and sent to the Herbarium of the Municipal Botanical Museum of Curitiba (# 363509). The stem bark of this plant species was cut and submitted to drying at room temperature for 14 days. The dry material was milled and then 334 g was mixed with a hydroalcoholic solution (30:70 water:ethanol, v/v) at a ratio of 1:5 (w/v). This mixture was homogenized for 8 days for exhaustive extraction (solvent exchanged every 2 days). The resulting solution was collected, filtered, concentrated, lyophilized and stored under refrigeration (4 °C) until the moment of use (70 g of dried crude extract (CE), yield of 21%, w/w). Fractions were obtained by extraction in a Soxhlet apparatus and 40.32 g of CE of *E. umbellata* was mixed with 20.16 g of kieselgel 60 silica (35–70 mesh, Merck®), which was conditioned in a filter paper bag and sealed. This material was extracted using a gradient of increasing polarity (hexane, chloroform, ethyl acetate and methanol (PA, Synth®)). The volume of the liquid extractant used for each solvent was 750 ml and the extraction time was 24 h. The solvents were completely removed under reduced pressure and low temperature to obtain a viscous material; subsequently, water was added to the concentrate extracts and freeze-dried. Finally the lyophilized materials (powder) that were obtained were stored under refrigeration (4 °C) for further analysis. The yield of the fractionation/dry process was as follows: 1.67% for the hexane fraction; 5.46% for the chloroform fraction; 0.84% for the ethyl acetate fraction; and 92.03% for the methanolic fraction.

Determination of total phenolics

The analysis of the total phenolic content of the hexane fractions (HF), chloroform fraction (CF), ethyl acetate fraction (EAF) and methanolic fraction (MF) was performed according to the Folin-Ciocalteau method. The crude extract and the fractions were re-suspended in their respective solvents at a concentration of 20 mg/ml. Aliquots of 500 μl were added to 10 ml flasks and the final volume was adjusted with their respective solvents at a concentration of 1 mg/ml; then 200 μl of these dilutions were transferred to the test tube and combined with 7 ml of distilled water and 0.5 ml of Folin-Ciocalteau reagent (Dinâmica®). After 30 s, 2.5 ml of 10.6% sodium carbonate solution (w/v, PA, Biotec®) was added. The tubes were homogenized and placed in a water bath at 50 °C for 5 min. After this period, the tubes were cooled and the readings were performed using a spectrophotometer (Genesy 10S UV-Vis, Thermo Scientific®) at 715 nm (Munhoz et al., 2014). The blank was prepared in the same way as the samples, replacing the fractions by distilled water. The analytical curve was obtained, in triplicates, with standard solutions of gallic acid (98% purity, Merck®) at concentrations of 50, 100, 200, 400, 600 and 800 μg/ml. The results were expressed in mg of gallic acid per g of sample.

Preparation of chitosan membranes

A chitosan solution (Sigma–Aldrich®/medium molecular weight (190–310 Da) and 75–85% degree of deacetylation) was prepared at a concentration of 1.5% (w/v) in 1% (v/v) acetic acid solution under constant agitation for 60 min. The material was subsequently filtered in sterile gauze and was added to 0.1% filtered sodium benzoate. It was homogenized for 20 min and then 1.5% of PEG 400 (w/w) and 0.2% of Tween 80 (w/w) were added, maintaining agitation for a further 20 min (ultrasound bath). The pH of the solution was adjusted to 5.5. From this solution, 7.5 g was poured into a plastic support (60 × 15 mm Petri dishes) and placed in an oven at 55 °C (±5 °C) for 4 h, to dry. After this period the supports were cooled in a desiccator and the membranes that had been formed were removed from the support, packed and sealed in plastic package (IM – inert membrane). For the membranes containing MF, the preparation steps were the same, but different percentages of freeze-dried MF (10% (M10MF), 50% (M50MF) and 100% (M100MF) in relation to the amount of chitosan) were added to the solution of PEG 400 and Tween 80, stirred, and subsequently spilled over the chitosan solution that was prepared as described above. A physical mixture (PM) of the components of the eligible formulation was prepared and used in the experiments. All membranes (packed and sealed) were stored for 72 h at a controlled environment (desiccator) before physicochemical analysis. For color measurements membranes were stored for 0, 7, 14, 21 and 28 days in the same conditions.

Characterization of chitosan membranes

The membranes were characterized regarding their morphology, porosity, density, thermal properties, crystallinity, color and chemical interactions. All analyses were performed in triplicate.

Scanning electron microscopy (SEM)

The morphological evaluation of the samples was performed by a Vega3 (Tescan®) scanning electron microscope. The samples were examined at an acceleration voltage of 5 kV. Magnifications up to 2500 were obtained. The membranes were coated with Au-Pd by the sputtering process.

Density

The densities of the membranes were measured by a AY220 balance (Shimadzu®) coupled with a density kit. The weights of the samples in air (m) (dried samples), and also immersed in a liquid of known density (m_a) at room temperature, were used to determine the density. The procedure was based on the Archimedes principle and density value was calculated by the equation described below (Song et al., 2014):

$$\rho_c = \frac{m}{m - m_a}\rho_F \quad (1)$$

where $\rho_F = 0.672\ g/cm^3$ – 25 °C (Hexane, PA, Vetec®).

Differential scanning calorimetry (DSC) and thermogravimetric analysis (TGA)

The DSC and TGA analyses were performed using LabSys Evo DSC/DTA (Setaram®) equipment. A heating rate of 10 °C/min in argon atmosphere (flow rate of 20 ml/min) was employed for all the samples. An amount of 7 mg of each sample was conditioned in hermetically sealed aluminum crucibles at a temperature range of 20–550 °C.

X-ray diffraction (XRD)

The XRD measurements of the membranes were performed using an Ultima IV X-ray diffractometer (Rigaku®) at room temperature using CuKα ($\lambda = 1.54$ Å) at 40 mA and 40 kV. The scattering range was 2θ from 5° to 60° and the scanning speed was 2°/min.

Fourier-transform infrared spectroscopy (FTIR)

The functional groups, and possible variation between them, were assessed by the FTIR technique using IR-Prestige 21 (Shimadzu®) equipment in the range of 4000–500 cm^{-1} with 32 scans/min and 4 cm^{-1} of resolution. The membranes were macerated with dry KBr (spectroscopic grade, Sigma–Aldrich®) at a ratio of 1:50 ratio by weight and then the pellets were prepared under a pressure of 80 kN.

Color measurements

The color values of the membranes were determined using a Cary 50 UV-Vis (Varian®) spectrophotometer equipped with a diffuse reflectance probe (Barrelino). The scale used for these measurements was the CIELAB $L^*a^*b^*$: $L^* = 0$ (black) to $L^* = 100$ (white), $-a^*$ (greenness) to $+a^*$(redness), and $-b^*$ (blueness) to $+b^*$(yellowness). The samples were placed upon a white plate with standard values of $L^* = 96.15$, $a^* = 0.12$ and $b^* = -1.75$. With a standard D65 light source and standard 2° observer, the $L^*a^*b^*$ coordinates were calculated using Color (Varian®) software. The color value changes related to storage time were measured on different days. The total color difference (ΔE^*) was determined (Wang et al., 2013) as follows:

$$\Delta E^* = \sqrt{\left(L^*_{standard} - L^*_{samples}\right)^2 + \left(a^*_{standard} - a^*_{samples}\right)^2 + \left(b^*_{standard} - b^*_{samples}\right)^2} \quad (2)$$

Chromatographic evaluation (LC–MS) of compounds in the MF of Euphorbia umbellata *and membranes*

The chromatographic profile of MF, the material that was released from IM, and the membranes incorporated with 10%, 50% and 100% of the fraction, were obtained using a previously published chromatographic condition (Minozzo et al., 2016).

In vitro *total phenolic release profile*

The release studies were performed according to the Alves et al. (2016) method with adaptations. A quantity of 10 ml of distilled water (pH = 6.8, room temperature) was added to each membrane (diameter: 60 mm, thickness: 105.50 ± 1.48 μm), and after each time interval the fluid was collected, lyophilized and stored until the analysis. The volume collected (10 ml) was suitable replaced on the plate. For the tests, the lyophilized samples were solubilized in MeOH (PA, Synth®). The analysis was performed according to the Folin-Ciocalteau method and the samples were analyzed by UV-Vis spectrophotometer at 715 nm. Total phenolic concentrations were calculated using calibration curves based on absorbance *versus* previously designed concentrations (Minozzo et al., 2016). The membrane samples (IM, M10MF, M50MF and M100MF) were tested in triplicate and the aliquots were collected at 0, 1, 2, 3, 4, 6 and 8 h of assay. The corresponding release profiles were represented by plots of the total phenolics that were released (mg gallic acid/g membrane extract) *versus* time. Mathematical models were applied to verify the mechanisms of drug release from the membranes, thus, *in vitro* drug release data were tested to fit (SigmaPlot software, version 10.0) Zero Order, Weibull and Korsmeyer-Peppas release kinetic models, in order to identify the one which presented the best adjusted coefficient of determination.

Zero order kinetics:

$$Q_t = Q_0 + K_0 t \quad (3)$$

where Q_t is the amount of drug dissolved in time t, Q_0 is the initial amount of drug in the solution (most times, $Q_0 = 0$) and K_0 is the zero order release constant.

Weibull:

$$\%D = 100 * \left[1 - e^{-(t/TD)/b}\right] \quad (4)$$

where $\%D$ = dissolved percentage, b = shape parameter, TD: time interval necessary to release 63.2% of the drug.

Korsmeyer-Peppas:

$$\%D = kt^n \quad (5)$$

where k = constant incorporating structural and geometric characteristic of the carrier, n is the release exponent, indicative of the mechanism of the drug release.

Antioxidant activity

Samples were obtained by applying the same procedure described in "*in vitro* total phenolic release profile" assay. For the tests, the lyophilized samples were solubilized in MeOH (PA, Synth®). Membrane samples (M10MF, M50MF and M100MF) were prepared in triplicate for each time of analysis and the results that were obtained were discounted from the results observed for the inert membranes (IM) at the same sampling time. The aliquots were collected at 0, 4, 8, 12 and 24 h of assay and the negative control was also performed with MeOH (without samples). The results were expressed as the concentration that inhibits 50% of the absorbance reading for the *in vitro* assays (IC_{50}). The IC_{50} values were determined by plotting the inhibition percentage *versus*

the final concentration of each sample. This inhibition (%) was calculated as:

$$\text{Inhibition}\ (\%) = \frac{\left(\text{ABS}_{\text{control}} - \text{ABS}_{\text{sample}}\right)}{\text{ABS}_{\text{CONTROL}}} * 100 \quad (6)$$

Inhibition expresses the oxidant amount scavenged by each sample. $\text{ABS}_{\text{control}}$ is the absorbance of the solution containing only the radical or reactive species and $\text{ABS}_{\text{sample}}$ is the absorbance value of the mixture of MF or quercetin solution and radical or reactive species. The absorbance measurement of both the control and the samples were followed by a blank (reaction medium without the oxidant).

DPPH• scavenging action:

The scavenging activity of the samples was tested in relation to 60 μM of DPPH• (2,2-diphenyl-1-picryl-hydrazyl, Sigma–Aldrich®), which was solubilized in absolute ethanol (Synth®) (Mi et al., 2003). The reaction medium was composed of 1, 5, 10, 20, 50, and 75 μl aliquots of sample and 300 μl of the DPPH• solution. The volume was completed with ethanol to 1000 μl. The mixture was incubated for 15 min at room temperature and protected from light. Activity was observed in terms of the decrease in absorbance at 531 nm. The reading was performed using a μQuant plate reader (Biotek®).

$ABTS^{\bullet+}$ scavenging action

The cationic $ABTS^{\bullet+}$ radical [2,2-azinobis (3-ethylbenzthiazoline sulfonic acid-6)] (Sigma–Aldrich®) was initially prepared by reacting 5 ml of ABTS aqueous solution (7 mM) with 88 μl of potassium persulphate (2.46 mM at room temperature and protected from light for a period of 12 to 16 h before use) (Mohamed and Wilson, 2012). Prior to the assay, the $ABTS^{\bullet+}$ solution was diluted with 10 mM of sodium phosphate buffer (1:20, v/v). Aliquots of 1, 5, 10, 20, 50, and 75 μl of the samples were added to Eppendorf tubes, along with 300 μl of $ABTS^{\bullet+}$ reagent, and the volume was completed to 1000 μl of reaction medium. The samples were incubated for 15 min, protected from light at room temperature ad read at 734 nm using a μQuant plate reader (Biotek®).

Antimicrobial activity

Agar diffusion

The membranes (IM, M10MF, M50MF and M100MF) were assessed in relation to pure colonies of *Escherichia coli* (ATCC 25922), *Staphylococcus aureus* (ATCC 25923), *Pseudomonas aeruginosa* (ATCC 27853) and *Candida albicans* (ATCC 90028), which were derived from recent cultures (18–24 h). Müeller-Hinton agar, in pH that was adjusted to 5.5 and 7.2, was used for the bacterial growth and amikacin was used as positive control. Müeller-Hinton agar containing 2% glucose and 0.5 μg/ml of methylene blue was used for the analysis of *C. albicans* (Chao, 2008), and 0.12% chlorhexidine was used as positive control. Saline solution (0.85% NaCl, w/v) was used as negative control. The inoculum was standardized in direct colony suspension equivalent to 0.5 of the McFarland scale ($1x10^8$ CFU/ml bacteria; $1x10^6$ CFU/ml fungi) (Siripatrawan and Harte, 2010). The membranes were cut into 5 mm diameter disks (thickness: 105.50 ± 1.48 μm), and placed on the inoculated agar (Tripathi et al., 2008). For the MF analyses disks with 5 mm diameter were impregnated with 60 μg, 300 μg, 600 μg, 1200 μg and 2400 μg, and placed on the inoculated media. The plates were incubated at 35 ± 2 °C, ambient air, for 24 h. After the incubation period, the plates were observed regarding the homogeneity of growth and the formation of growth inhibition zones. The diameter of the halo was determined and inhibition halos larger than 8 mm were considered positive (Prashanth et al., 2002).

Determination of the minimum inhibitory concentration (MIC)

The samples were obtained according to the procedure described in "*in vitro* total phenolic release profile" assay. The MIC method was performed in 96 well plates. The microorganisms were grown in Müeller-Hilton broth for 6 h. After this period, in order to obtain the final concentrations of 1.5, 1.0, 0.5, 0.25 and 0.125 mg/ml of released compounds from the membrane, aliquots of each sample (6 mg/ml) were added to each well, which contained 10 μl of microorganisms and the volume was completed with Müeller-Hinton broth up to 200 μl. The culture medium and the microorganism were prepared as negative and positive controls respectively. After 24 h incubation at 35 ± 2 °C, ambient air, the MIC of each sample was determined by quantifying the optical density in a μQuant plate reader (Biotek®) at 630 nm, comparing the data obtained for the samples and the nutrient medium (negative control). The lowest concentration of the samples capable of inhibiting microbial growth was regarded as the MIC (Zhang and Kosaraju, 2007).

Statistical analysis

The experimental data were expressed as mean ± standard deviation (SD) or mean ± standard error of the mean (SE). The data from the color and antioxidant analyses were assessed by analysis of variance (ANOVA) and Tukey's test. The data were analyzed using Origin 9.0 software with a 5% significance level ($p < 0.05$). The linear correlation tests were performed using the Statistica 8.0 program (StatSoft Software®).

Results and discussion

In order to obtain a chitosan membrane incorporated with plant extract rich in phenolic compounds, as well as providing adequate homogeneity, resistance to manipulation (pelled from the casting plates), release of compounds, antimicrobial, and antioxidant activities, the phenolic compound content in the fractions (*n*-hexane, chloroform, ethyl acetate and methanol) from the bark CE of *E. umbellata* was initially quantified. UV–vis spectrometry was used for this purpose and three analytical curves of gallic acid (50, 100, 200, 400, 600 and 800 μg/ml) with adjustments in the assessed range ($r^2 = 0.9986$) were determined.

The MF (318.64 ± 0.64 mg/g of fraction, expressed in gallic acid) showed higher total phenolic values when compared with the other evaluated fractions. These data were consistent with those published previously, which evaluated the MF of *E. umbellata* (using the LC–MS technique) and which confirmed the majority presence of phenolic compounds in this material, including gallic acid, ellagic acid and flavonoids (Minozzo et al., 2016). Another study which assessed the extract of the bark of this species using HPLC-DAD determined that the material was rich in phenolic compounds such as flavonoids (Munhoz et al., 2014). Other species of *Euphorbia* have presented phenolic compounds in their extracts, which confirm the data obtained in the present study. More than 84% of the phenolics identified in extracts of *Euphorbia supina* were glycosylated derivatives of flavonoids (Kittur et al., 2003). Similarly, a study of the most polar fractions (methanolic and acetonic) of the species *Euphorbia tirucalli* showed the presence of total phenolic compounds (Zhang and Zhao, 2015).

Thus, the MF was selected to be evaluated as the active component of a chitosan formulation. Experiments were initially conducted to decide the excipients and their concentrations in the formulation, as well as the adequate preparation mode, which are presented in Table 1.

During membranes development process, authors observed that the PEG 400 (plasticizer agent) added to the formulation increased

Table 1
Factors evaluated in the process of the development of chitosan membranes.

Factor	Material	Criteria evaluated
Chitosan	Medium molecular weight (Sigma–Aldrich®, 448877)	1%, 1.5%, 2%, and 3% (w/w)
	Low molecular weight (Sigma–Aldrich®, 448869)	1% (w/w)
Extract/fraction	Methanolic fraction (freeze-dried)	10%, 30%, 50%, 80%, 100%, and 110% (w/w)[a]
Excipients	Sodium benzoate	0.1% (w/v)
	Glycerin	0%, 2%, 3%, 4% and 5% (w/w)[a]
	PVP	5% (w/w)[a]
	TWEEN 80®	0.2% (w/w)[a]
	PEG 400	1.5% (w/w)[a]
	Acetic acid	1%, and 2% (v/v)
Form	Petri dishes	Glass
		Plastic
Casting	Time (h)	1, 4, 6, and 18
	Temperature (°C)	65, 60, and 55
Wash	Sodium hydroxide solution 2% (w/v)	4 °C, and room temperature
	Distilled water	4 °C, and room temperature

[a] Relation to the amount of chitosan.

the resistance to manipulation (pelled from the casting plates) of the membranes (product). Furthermore, the addition of this excipient to the formulation was required to form pores in the membrane, as well as it has been described in some studies (Siripatrawan and Harte, 2010; Wang et al., 2013). Consequently, the authors concluded that this component was important for the product and the expected release profile.

It was also realized that the addition of Tween 80 helped into the complete solubilization of MF in the membrane formula, since the authors observed that the extract was not completely soluble in the formulation. In order to solve this problem, the addition of surfactant was proposed, in accordance with some previous studies (Rubilar et al., 2013). These two components (Tween and PEG 400), as well as the other excipients of the proposed formulation, were added in the same amounts for all samples. Once all parameters were evaluated, the best components had been chosen for the formulation, and the most appropriate preparation mode had been selected to obtain homogeneous membranes (lack of apparent precipitation), and allowing adequate manipulation, the membranes were prepared and the physicochemical characterizations were performed.

Fig. 1 presents the morphology of the membranes prepared with different proportions of MF in plastic support. Superficial pores could be observed on the surface of the inert membrane (with average diameters of around 1 μm) (Fig. 1A) and the same behavior was observed in the sample with 10% of MF (Fig. 1B). For the M50MF and M100MF membranes (Fig. 1C and 1D), was observed an increased superficial pore size (around 2 μm). These different morphological properties must be related to the variation in the relative difference in the solubility parameter between the MF content, the chitosan and the solvent (Epure et al., 2011) since the same solvent (acetic acid) was used for the preparation of all the membranes. Considering Hansen's three component definition ($\Delta\delta$), which contributions of dispersion forces (δd), dipolar interactions (δp) and hydrogen-bond capacity (δh) describe the behavior of $\Delta\delta$, it is able to conclude that the addition of MF into the chitosan membrane can induce interactions between the amino groups of chitosan and the oxygen present in the phenolic compounds in the MF, thereby increasing the δd, δp and δh values (Epure et al., 2011; Rubilar et al., 2013). As $\Delta\delta$ values increase, the chitosan network fails to retain its individuality and undergoes aggregation into open clusters, widening the voids between the subunits and resulting in larger pores (Banerjee et al., 2002).

The hypothesis that the phenolic compounds extracted fitted into the polymeric matrix by a hydrogen interaction, or covalent bonding with intermolecular amino groups of chitosan, also can help to explain the results observed for the density test. Although the effect of the MF addition on the density was not significantly ($p < 0.05$), density of the membranes still slightly increased with the enhancing of MF amount (Table 2) (Siripatrawan and Harte, 2010; Wang et al., 2013).

The interaction between the previously proposed polymeric matrix and the compounds presented in MF were confirmed by the DSC and TGA results (Fig. 2A and B). The first phenomenon that was observed was a wide endothermic event with a peak temperature in the 70–100 °C range. Peak temperatures for all the samples, as well as the enthalpy energy (ΔH_{endo}) of this transition are listed in Table 2. This transition was attributed to the evaporation of bound water. How it is well known, polysaccharides usually have a strong affinity for water and this hydration property depends on the primary and supra-molecular structures. Furthermore, the presence of bound water also has a strong influence on the overall polymorphic nature of the macromolecules (Ramos-Tejada et al., 2002). The decrease in ΔH_{endo} with increasing MF content is indicative that the chemical interactions were altered, since the amino groups of chitosan can interact with the oxygen molecules present in the MF compounds and are less available to form bonds with water molecules. This phenomenon was observed in a chitosan matrix loaded with catechin (Torreggiani et al., 2008).

The second event showed an exothermic transition at 270 °C, as well as enthalpy energy (ΔH_{exo}) variation between samples. This transition was only observed for IM and M10MF samples; whereas M50MF and M100MF samples showed a ΔH_{exo} that was not significant. This difference in the thermal characteristic reinforces the proposal of regarding the interaction between the amine groups of chitosan and the phenolic compounds in the MF (Curcio et al., 2009; Siripatrawan and Harte, 2010).

Fig. 2B shows the TGA results, in which two decomposition steps can be observed. The first degradation stage was at ~100 °C with a mass loss of 18% for IM and 12% for M100MF, which was attributed to the evaporation of water contained in the polymer. The second stage occurred at ~120–450 °C, which was attributed to the dehydration of the saccharide rings and the depolymerization and decomposition of the acetylated and deacetylated units in the samples (Peniche et al., 1992; Zhang and Zhao, 2015). The amount of remaining polymer at 550 °C for the different samples is shown in Table 2. The M100MF and M50MF samples had higher remaining amounts, with a solid residue of approximately 22% of the initial mass. Because the same amounts of sample were added in the TGA experiment to avoid systematic errors, and the chitosan used in the sample preparation possessed the same degree of acetylation, it can be inferred that higher amounts of water were present in the IM and M10MF samples. This reinforces the data obtained by DSC, which showed higher ΔH_{endo} values for the latter two samples compared with the M50MF and M100MF samples (covalent and hydrogen interactions between the polymeric matrix and the phenolic compounds decrease the affinity of chitosan membranes toward water) (Siripatrawan and Harte, 2010) (Table 2). Furthermore, the increase in the solid content in the formulations (M50MF and M100MF samples) could have contributed to the results that were obtained.

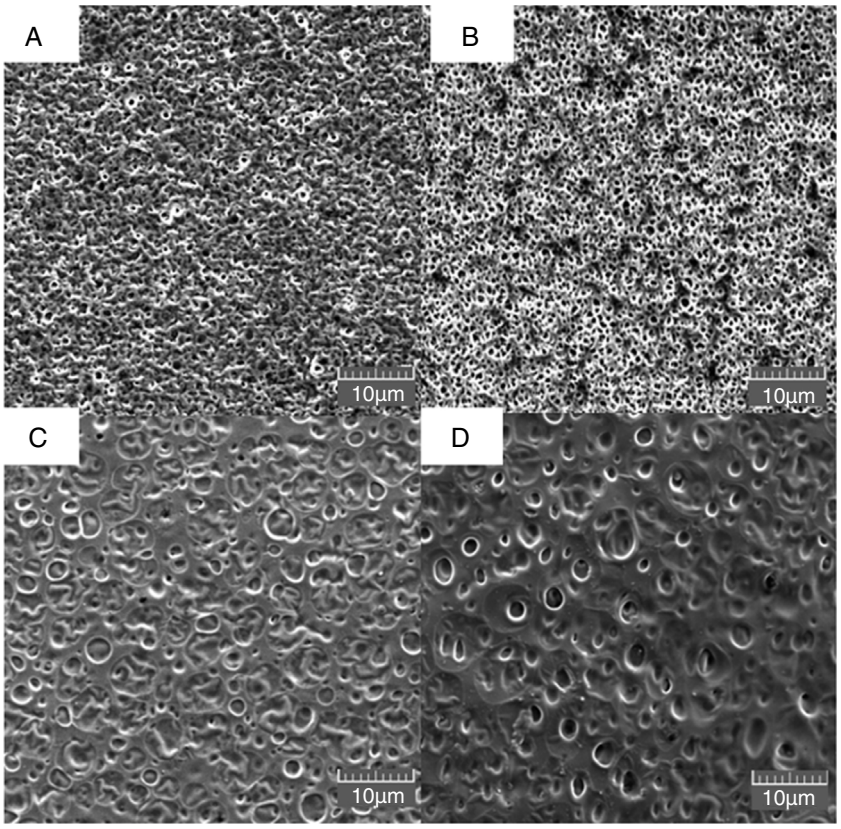

Fig. 1. Morphology of membrane surfaces evaluated by scanning electron microscopy with different extract concentrations. (A) IM, (B) M10MF, (C) M50MF, and (D) M100MF.

Table 2
Density of chitosan membranes incorporated with MF, and thermal data obtained by DSC/TGA techniques.

Sample	Density (g/cm^3)	Thermal data				Residual mass (%)
		Endothermic transition		Exothermic transition		
		Position (°C)	ΔH_{endo} (mW/mg)	Position (°C)	ΔH_{exo} (mW/mg)	
IM	1.25 ± 0.02[a]	73.3	98.42	269.91	6.02	18.00
M10MF	1.30 ± 0.02[a]	69.4	94.03	272.59	5.87	18.00
M50MF	1.35 ± 0.03[a]	65.1	77.15	256.48	0.62	21.00
M100MF	1.44 ± 0.04[a]	61.4	78.85	251.97	0.80	23.00

Values represent the mean ± standard deviation of the replicates. One-way ANOVA followed by Tukey's post-test. Two values followed by the same letter in the same column are not significantly different ($p < 0.05$) through the Tukey's multiple range test.

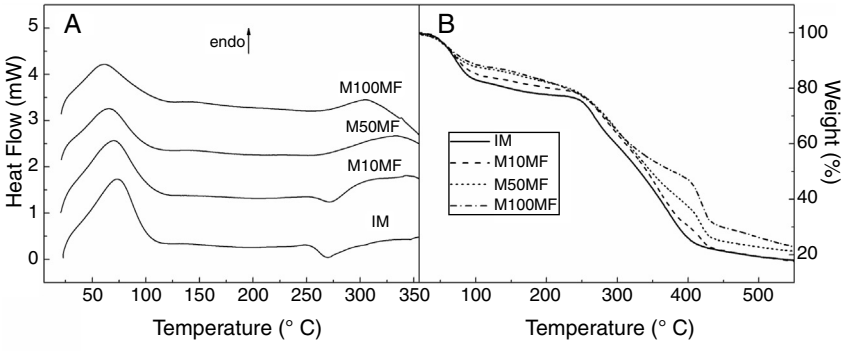

Fig. 2. (A) DSC results for M100MF, M50MF, M10MF and IM (highlighting the temperature range: 20–350 °C); (B) mass loss curves for M100MF, M50MF, M10MF and IM. DSC and mass loss curves were performed in the temperature range of 20–550 °C.

Fig. 3A presents the X-ray diffraction patterns of the IM sample, which showed a diffraction pattern with two halos centered at ~8° and ~20° (Fig. 3A). The first halo was attributed to the integration of water molecules in the crystal lattice (form I), and the halo located at 20° was attributed to the regular crystal lattice of chitosan (Zhang et al., 2006; Epure et al., 2011; Rubilar et al., 2013). The samples with increasing levels of MF content showed a decrease in the intensity and displacement of the crystalline

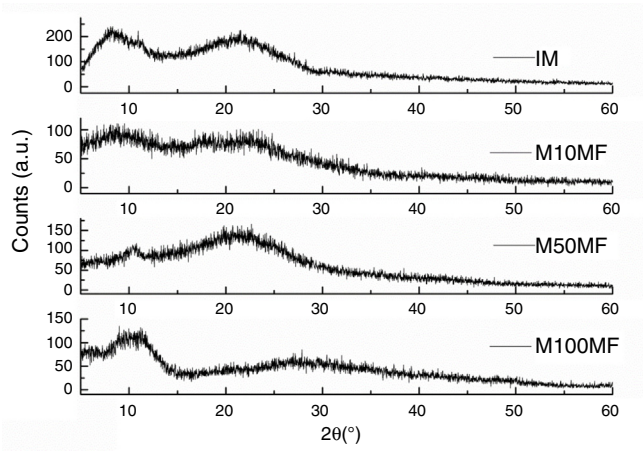

Fig. 3. X-ray diffractograms of: IM, M10MF, M50MF, M100MF samples, highlighting the decrease in the intensity and displacement of the crystalline halo centered at ~20°. Analysis conditions: scattering range was 2θ from 5° to 60° and the scanning speed was 2°/min.

halo centered at ~20° in the chitosan membrane. This decrease in intensity can be attributed to enhance the intermolecular interactions between chitosan polymer chain and polyphenolic compounds of MF, and was previously described by Siripatrawan and Harte (2010) (Fig. 3B). Furthermore Vieira and Beppu (2006) also described a decrease in the halo intensity due the presence of compounds between the chitosan chains, decreasing the packing characteristic and enhancing the amorphous nature of the chitosan membrane.

Fig. 4A presents the FTIR spectra for all studied samples, as well as the physical mixture of chitosan and MF for comparing. As the IM spectrum shows, the broad band centered at ~3400 cm^{-1} corresponded to combined peaks of OH, NH stretching and intramolecular hydrogen bonding. The band centered at ~2900 cm^{-1} was attributed to the C—H stretching of the polymer backbone (Ferreira et al., 2014). The NH_2 scissoring vibration of the primary amide was observed at 1559 cm^{-1}. The 1460 cm^{-1} was due to the CH_2 bending and was related to the rearrangement of the hydrogen bonds in an orientation more favorable to the —OH groups in chitosan, 1350 cm^{-1}, which is related to the axial deformation of CN in the amino groups, 1093 and 1031 cm^{-1} (skeletal vibrations involving the C—O stretching), which are characteristic of the chitosan saccharide structure. Regarding MF: the broad band centered at 3390 cm^{-1} was attributed to the —OH stretching; the 2927 cm^{-1} was –CH stretching; the 1712 cm^{-1} was C=O grouping of carboxylic acid; 1627 cm^{-1} was aromatic ring stretching; 1400–1000 cm^{-1} was attributed to C—O stretching from phenol; and CO—C was attributed to bending and C—OH stretching (Kasaai, 2008; Mayachiew and Devahastin, 2010; Ferreira et al., 2014).

An important change that was observed in the membranes with MF was the new narrow band at 1715 cm^{-1}, which was attributed to an ester linkage that may have been related to the more intense interaction of the chitosan matrix and MF (Fig. 4B) (Mayachiew and Devahastin, 2010). It was also possible to observe a band at ~1660 cm^{-1}, which was related to the stretching of the C=O of amide grouping. These observations may suggest an interaction between the amine groups of chitosan and the acid groups of the phenolic compounds (particularly gallic acid and ellagic acid) in MF (Fig. 4B).

Similarly, the color data regarding IM, and the membranes with different concentrations of MF measured at different times proved that there are interactions between the chitosan and the compounds present in MF. The results were expressed according to the CIELAB scale (Supplementary Material).

The increase in the concentration of MF added to the membranes resulted in a change in coloration of the membranes to a darker brown color. The values for a^*, b^*, L^* and total color (ΔE) for the different evaluated membranes showed significant heterogeneity among samples and statistical differences ($p < 0.05$, Tukey's test).

Regarding storage time, it was observed that the membranes with the highest incorporated concentrations of MF experienced a higher degree of darkening over time. Studies have shown that chitosan membranes incorporated with extracts containing phenolic compounds showed similar behavior (Mohammed-Ziegler and Billes, 2002; Quideau et al., 2011; Kanatt et al., 2012), and the characteristic of the darkening of phenolic compounds added to polymer matrices has also been highlighted in other studies (Soares et al., 1997; Leceta et al., 2013; Alves et al., 2016).

The alteration of a^*, b^* and ΔE with storage time could indicate that the samples possessed a higher reducing end content or less steric hindrance in line with increasing MF content. This may have been due to the condensation of amine groups (from chitosan) with carboxylic groups (from MF). Phenolic compounds, such as gallic acid, contain carboxylic groups, which could interact with chitosan according to the reaction described above. This interaction explains the DSC results, which demonstrated that the higher the MF content, the lower the hydration of the membrane. This interaction was also supported by the XRD and FTIR results.

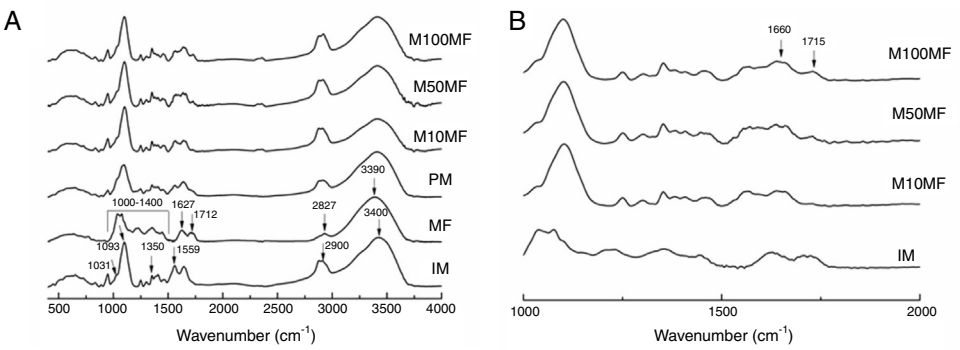

Fig. 4. (A) Infrared spectra of different membranes containing MF (M100MF, M50MF and M10MF), of physical mixture (PM), of methanolic fraction (MF), and of inert membrane (without MF, IM). The dashed vertical lines mark the IM bands and the continuous vertical lines mark the MF bands (analysis conditions: range of 4000–500 cm^{-1} with 32 scans/min and 4 cm^{-1} of resolution). (B) highlighting the wavenumber range: 500–2000 cm^{-1}.

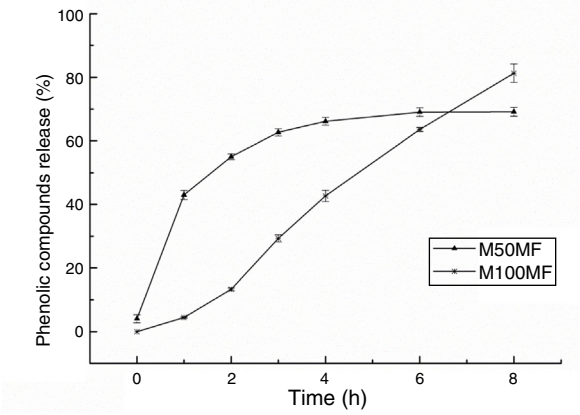

Fig. 5. *In vitro* release of total phenolic compounds from M50MF and M100MF samples ($n = 3$) performed according to the Folin-Ciocalteau method.

After the physicochemical characterization of the membranes incorporated with different concentrations of the MF, and the qualification of the compounds present in this fraction, the next step was to determine the quantification of phenolic compounds released from the membrane, as well as the antioxidant and antimicrobial potential of this material. Although numerous studies have assessed the antioxidant and antimicrobial activity of plant extracts that are rich in phenolic compounds (Pellegrini et al., 1998), few have evaluated the antioxidant potential associated with the capacity to release extracts from polymeric materials (Pfaller et al., 2004). The analysis of the material released from the membranes incorporated with different amounts of MF presented a chromatographic profile that was similar to that previously reported for the methanolic fraction of *E. umbellata* (Minozzo et al., 2016).

Studies have shown that phenolic compounds, like those derived from catechol nucleus, hydrolysable tannins and gallotannins such as those present in the MF, have been featured in research because of the variety of biological actions that they perform (Silva et al., 2011; CLSI, 2016).

The amount of total phenolic compounds released from the chitosan matrix showed different profiles of these substances according to the concentration of MF added to the membrane formulations. For the M50MF sample, a fast release of the total phenolic compounds in the first hour of the test was observed (137.01 ± 4.54 mg/g, 42.99%) and the release of the phenolic compounds was controlled, reaching a plateau (210.74 ± 3.83 mg/g, 66.14%) after 4 h.

The release of phenolic compounds from the membranes with 100% MF (M100MF) demonstrated a different behavior when compared with the M50MF sample. The amount of phenolic compounds released was slower, and in the first hour only 4.43% (14.11 ± 0.67 mg/g) was released from the membrane. However, there was a controlled profile during the test, releasing 81.29% (259.04 ± 9.18 mg/g) at the end of 8 h, although a plateau was not observed during this time (Fig. 5).

The membranes were analyzed using three models in order to better characterize the release profile of phenolic compounds with a high degree of correlation; it was observed that the compounds were released by different mechanisms according to their levels in the membrane (Table 3) (Costa and Lobo, 2001). Using the Weibull model, the results of the regression analysis indicated that the release of phenolic compounds from the membrane was satisfactorily described by this model. The results showed that the release of the phenolic compounds from the M50MF sample occurred by Fickian diffusion (b values lower than 0.75), which is characterized by a high rate of water diffusion to the polymeric matrix and a low rate of polymeric relaxation.

Furthermore, as it is shown in Table 3, the b value for the M100MF sample was greater than 1.0, indicating that the release of phenolic compounds occurred by a complex mechanism in which several processes occurred simultaneously.

The Korsmeyer-Peppas model also demonstrated that the release of phenolic compounds from the M50MF sample occurred by diffusion ($n < 0.5$), and in the case of the M100MF sample it occurred by super case-II transport mechanism, which indicates that the release of phenolic compounds occurred by both swelling and diffusion – ($n \geq 1$, Table 3). It was observed that the higher proportion of phenolic compounds in the M100MF sample reduced the rate of release due to the interaction between the phenolic compounds and chitosan. This interaction results in smaller amounts of hydrophilic groups in the polymer matrix, showing a decrease in the active compounds diffusional path and a consequent delay in the release rate.

Drug dissolution from pharmaceutical dosage forms that do not disaggregate and release the drug slowly (assuming that area does not change and no equilibrium conditions are obtained) can be represented by the Zero Order Kinetics. As it is possible to observe in Fig. 5 and Table 3, only sample M100FM showed correlation with this model and the membrane followed this release profile (same amount of phenolic compounds by unit of time, with the exception of the initial period – first 2 h of release) that is the ideal method of drug release in order to achieve a pharmacological prolonged action.

Thus, the different release profiles of the samples may have been due to the interactions between the amine groups of chitosan and the carboxyl groups of the phenolic compounds. The M50MF sample (which contained a lower quantity of phenolic compounds than the M100MF sample) presented a lower level of chemical interaction, allowing a higher hydration of the chitosan matrix, with consequently more control of the phenolic compounds released by the polysaccharide. On the other hand, the M100MF sample presented higher levels of chemical interaction between chitosan and the phenolic compounds, causing a reduction in membrane hydration and reducing the amount of compounds released at the beginning of the test. High levels of interaction also reduce the ability of the chitosan to control the release of phenolic compounds, which usually occurs after polysaccharide hydration and swelling.

Table 3
R^2 adjusted values and exponent release n and b of the release of phenolic compounds from the membranes when fitted to Zero order, Korsmeyer-Peppas and Weibull models. Calculations performed according to equations reported by Costa and Lobo (2001).

Sample	Mathematic Model						
	Korsmeyer-Peppas			Weibull			Zero Order
	R^2_{adj}	n	Mechanism	R^2_{adj}	b	Mechanism	R^2_{adj}
M50FM	0.9876	0.3422	Fickian diffusion	0.9965	0.4930	Fickian diffusion	0.8008
M100FM	0.9857	1.2516	Super case-II transport	0.9984	1.4248	Complex mechanism	0.9781

R^2_{adj} – adjusted coefficient of determination; n – exponent release; b – indicative of release mechanism.

Table 4
Inhibitory potential of chitosan membranes impregnated with methanolic fraction of *E. umbellata*.

Sample	pH	*C. albicans* (mm)	*S. aureus* (mm)	*P. aeruginosa* (mm)	*E. coli* (mm)
IM	7.2	0	0	0	0
	5.5	0	0	0	0
M10MF	7.2	0	0	0	0
	5.5	0	0	8	0
M50MF	7.2	0	0	0	0
	5.5	0	7.5	10	0
M100MF	7.2	7	0	0	0
	5.5	6.5	13	10	0
Positive control	7.2	17	24	31	30
	5.5	22	23	33	30
Negative control	7.2	0	0	0	0
	5.5	0	0	0	0
MF[a]	7.2	0	9	7	6
	5.5	0	10	7	8

[a] Disks containing 1200 μg of MF.

These results may reinforce the data discussed previously. The amount of total phenolics released from the M10MF sample was very small and was not quantified.

The antioxidant activity of the MF released from the chitosan membranes was evaluated and the M50MF and M100MF membranes had higher levels of antioxidant activity (up than 70%) compared to the M10MF membrane and the inert membrane (IM). After 24 h of the experiment, all the evaluated samples showed no increase in the % of inhibition. The DPPH• test results were consistent with the data obtained by ABTS•+. The determination of the IC_{50} of the membranes incorporated with methanolic fraction of *E. umbellata* for the DPPH• and ABTS•+ tests showed higher antioxidant potential for the M100MF samples (DPPH• IC_{50}: $280 \pm 20\ \mu g\ ml^{-1}$ and ABTS•+ IC_{50}: $273 \pm 6\ \mu g\ ml^{-1}$). This result was replicated in the other samples, which showed higher IC_{50} values as the concentration of extract was decreased in the membranes. The M10MF membrane presented values of 29.31% inhibition of DPPH• and 37.5% for ABTS•+ (it was not possible to calculate the IC_{50} for these methodologies). The IM sample showed no inhibition in relation to the two tested radicals, which was expected. The results showed statistically significant difference ($p < 0.05$, Tukey's test) at times of 0 and 24 h for both tests. The IC_{50} for the MF released from the samples was lower than the value observed for the non-incorporated fraction, suggesting that phenolic compounds were not immediately released from the membranes, at least under the tested conditions, and confirming the previous data (Table 3).

Kanatt et al. (2012) evaluated the antioxidant activity of chitosan membranes incorporated with pomegranate extract and mint extract at different times and found that they showed an increase in antioxidant activity over time, reaching approximately 80% inhibition in 24 h. Similarly, Mayachiew and Devahastin (2010) evaluated the antioxidant activity of chitosan membranes incorporated with Indian gooseberry extract and found that the scavenging activity of the radicals occurred quickly in the first 8 h of the experiment and more steadily during a second period between 8 and 24 h of the experiment, which corroborates the data obtained in the present study.

The microbial inhibition by the M10MF, M50MF and M100MF membranes occurred in a concentration-dependent way. It was also possible to determine the inhibition of microbial growth (*S. aureus* and *P. aeruginosa*), especially at a pH of 5.5 (higher exclusion zone area: 13 mm), when compared to the controls (positive control – higher exclusion zone area: 33 mm, negative control – no presence of exclusion zone). The inhibition of cell growth occurred not only in the peripheral zone of the disk but also on the disk area, making it possible to predict that the pH of 5.5 may have facilitated the spread of the compounds from the formulation to the agar (culture medium) (Table 4). This result was interesting because this pH mimics the physiological condition of the pH of inflamed skin, indicating that in these conditions there would be greater release of the compounds to the skin, with a consequent development of antimicrobial actions (Nascimento et al., 2000). It was also observed that the inert membrane (IM – blank sample) did not present inhibition of microbial growth. Microbiological activity was possibly not observed in relation to the IM sample because, as described by Goy et al. (2009), for chitosan acts as an antimicrobial agent it is necessary that this polymer is solubilized in the media so that it can act properly. The MIC results for the tested load membrane samples confirmed that none of the tested samples showed activity in relation to *E. coli*, and the value of 0.125 mg/ml, mainly for *S. aureus*, was determined. MF presented values of the MIC of 0.125 mg/ml for *S. aureus* and 1 mg/ml for *E. coli* (was not possible to determine the MIC values of MF to *P. aeruginosa* and *C. albicans*).

As the dimensions of the membranes did not vary statistically the amount of MF present in the samples can explain the higher amount of phenolic compounds released from the membranes with 100% MF, and the best antioxidant and microbial results obtained for this sample.

This study demonstrated that an active membrane from chitosan could be achieved by incorporating a fraction rich in phenolic compounds (MF from *E. umbellata*). The addition of increasing amounts of MF changed some physicochemical characteristics of the chitosan matrix due to the presence of higher amounts of phenolic compounds. These changes were confirmed by FTIR, DRX, SEM, DSC and TGA analyses and they made possible to conclude that the interactions between the amine groups of the chitosan matrix and the polar compounds present in the phenolic fraction were responsible for the changes. The analyses of color and density corroborated the data obtained by the previous physicochemical analyses. Although an interaction occurred between the chitosan matrix and the polar compounds of the MF, the release study proved that the active compounds were suitable controlled released from the matrix but *via* different mechanisms. This release profile allowed the chitosan-MF membranes to show antioxidant and antimicrobial activity in a concentration-dependent way. These characteristics suggest the great potential of the obtained matrix to be used as medicinal membrane; however, several further studies need to be performed before using this new material for future applications as medicine.

Ethical disclosures

Protection of human and animal subjects. The authors declare that no experiments were performed on humans or animals for this study.

Confidentiality of data. The authors declare that no patient data appear in this article.

Right to privacy and informed consent. The authors declare that no patient data appear in this article.

Authors' contributions

BML (MA student) performed all the tests presented in this article, worked on the characterization analyses and helped to write the article. AN was responsible for helping in the characterization tests and for guiding the analyses of physicochemical data, as well

as contributing to the writing of the article. SRFS assisted in the performance of the physicochemical tests. JCRV was responsible for support in performing and analyzing the antioxidant assays, as well as correcting the final version. BRM helped to perform the antioxidant analyses and in the discussion of the results. ASJ, VEKP and JVG (undergraduate students) helped to perform the biological tests. LAE was responsible for support in the antimicrobial assays, as well as correcting the final version. FLB was responsible for obtaining financial support, writing the paper, coordinating the research work and providing the material for the research.

Conflicts of interest

The authors declare no conflicts of interest.

Acknowledgments

The authors are grateful to Professor Fernanda Malaquias Barbosa for text correction as well as the National Center for Natural Products Research (NCNPR – University of Mississippi, USA) for technical support. This study was financially supported by Fundação Araucária (Research Grant 490/2014 and 234/2014), CNPq (Process 232511/2014-4) and CAPES by a scholarship.

Appendix A. Supplementary data

Supplementary data associated with this article can be found, in the online version, at doi:10.1016/j.bjp.2018.05.001.

References

Abdel-Rahman, R.M., Abdel-Mohsen, A.M., Hrdina, R., Burgert, L., Fohlerova, Z., Pavlinák, D., Sayed, O.N., Jancar, J., 2016. Wound dressing based on chitosan/hyaluronan/nonwoven fabrics: preparation, characterization and medical applications. Int. J. Biol. Macromol. 89, 725–736.

Alves, A.C.S., Mainardes, R.M., Khalil, N.M., 2016. Nanoencapsulation of gallic acid and evaluation of its cytotoxicity and antioxidant activity. Mater. Sci. Eng. C 60, 126–134.

Banerjee, T., Mitra, S., Singh, A.K., Sharma, R.K., Maitra, A., 2002. Preparation, characterization and biodistribution of ultrafine chitosan nanoparticles. Int. J. Pharm. 243, 93–105.

Benhabiles, M.S., Salah, R., Lounici, H., Drouiche, N., Goosen, M.F.A., Mameri, N., 2012. Antibacterial activity of chitin, chitosan and its oligomers prepared from shrimp shell waste. Food Hydrocolloid. 29, 48–56.

Bernkop-Schnürch, A., Dünnhaupt, S., 2012. Chitosan-based drug delivery systems. Eur. J. Pharm. Biopharm. 81, 463–469.

Chao, A.-C., 2008. Preparation of porous chitosan/GPTMS hybrid membrane and its application in affinity sorption for tyrosinase purification with *Agaricus bisporus*. J. Membr. Sci. 311, 306–3018.

CLSI, 2016. Performance Standards for Antimicrobial Susceptibility, Testing 26th ed. CLSI supplement. M100S. Clinical and Laboratory Standards Institute, Wayne, PA.

Coqueiro, D.S.O., Di Piero, R.M., 2011. Atividade de quitosanas com diferentes pesos moleculares sobre *Alternaria solani*. Arq. Inst. Biol. 78, 459–463.

Costa, P., Lobo, J.M.S., 2001. Modeling and comparison of dissolution profiles. Eur. J. Pharm. Sci. 13, 123–133.

Curcio, M., Puoci, F., Iemma, F., Parisi, O.I., Cirillo, G., Spizzirri, U.G., Picci, N., 2009. Covalent insertion of antioxidant molecules on chitosan by a free radical grafting procedure. J. Agric. Food Chem. 57, 5933–5938.

Denkbas, E.B., Ottenbrite, R.M., 2006. Perspectives on: chitosan delivery systems based on their geometries. J. Bioact. Compat. Pol. 21, 351–368.

Dias, K.B., Silva, D.P., Ferreira, L.A., Fidelis, R.R., Costa, J.L., Silva, A.L.L., Scheidt, G.N., 2013. Chitin and chitosan: characteristics, uses and production current perspectives. J. Biotechnol. Biodivers. 4, 184–191.

Epure, V., Griffon, M., Pollet, E., Avérous, L., 2011. Structure and properties of glycerol plasticized chitosan obtained by mechanical kneading. Carbohydr. Polym. 83, 947–952.

Ferreira, A.S., Nunes, C., Castro, A., Ferreira, P., Coimbra, M.A., 2014. Influence of grape pomace extract incorporation on chitosan films properties. Carbohydr. Polym. 113, 490–499.

Freitas, R.M., Spin-Neto, R., Spolidório, L.C., Campana-Filho, S.P., Marcantonio, R.A.C., MarcantonioJr., E., 2011. Different molecular weight chitosan-based membranes for tissue regeneration. Materials 4, 380–389.

Goy, R.C., Britto, D de, Assis, O.B.G.A., 2009. Review of the antimicrobial activity of chitosan. Polímeros 19, 241–247.

Kasaai, M.R., 2008. A review of several reported procedures to determine the degree of *N*-acetylation of chitin and chitosan using infrared spectroscopy. Carbohydr. Polym. 71, 497–508.

Kanatt, S.R., Rao, M.S., Chawla, S.P., Sharma, A., 2012. Active chitosan-polyvinyl alcohol films with natural extracts. Food Hydrocolloid. 29, 290–297.

Kittur, F.S., Vishu Kumar, A.B., Tharanathan, R.N., 2003. Low molecular weight chitosans-preparation by depolymerization with *Aspergilus niger* pectinase, and characterization. Carbohydr. Res. 338, 1283–1290.

Leceta, I., Guerrero, P., Caba, K., 2013. Functional properties of chitosan-based films. Carbohydr. Polym. 93, 339–346.

Martel-Estrada, S.A., Rodriguez-Espinoza, B., Santos-Rodríguez, E., Jiménez-Veja, F., García-Casillas, P.E., Martínez-Pérez, C.A., Armendáriz, I.O., 2015. Biocompatibility of chitosan/*Mimosa tenuiflora* scaffolds for tissue engineering. J. Alloys Compd. 643, S119–S123.

Mayachiew, P., Devahastin, S., 2010. Effects of drying methods and conditions on release characteristics of edible chitosan films enriched with Indian gooseberry extract. Food Chem. 118, 594–601.

Mi, F.L., Wu, Y.B., Shyu, S.S., Chao, A.C., Lai, J.Y., Su, C.C., 2003. Asymmetric chitosan membranes prepared by dry/wet phase separation: a new type of wound dressing for controlled antibacterial release. J. Membr. Sci. 212, 237–254.

Minozzo, B.R., Lemes, B.M., Justo, A.S., Lara, J.E., Petry, V.E.K., Fernandes, D., Belló, C., Vellosa, J.C.R., Campagnoli, E.D., Nunes, O.C., Kitagawa, R.Z., Avula, B., Khan, I.A., Beltrame, F.L., 2016. Anti-ulcer mechanisms of polyphenols extract of *Euphorbia umbellata* (Pax) Bruyns (Euphorbiaceae). J. Ethnopharmacol. 191, 29–40.

Mohamed, M.H., Wilson, L.D., 2012. Porous copolymer resins: tuning pore structure and surface area with non-reactive porogens. Nanomaterials 2, 163–186.

Mohammed-Ziegler, I., Billes, F., 2002. Vibrational spectroscopic calculations on pyrogallol and gallic acid. J. Mol. Struct. 618, 259–265.

Munhoz, A.C.M., Minozzo, B.R., Cruz, L.S., Oliveira, T.L., Machado, W.M., Pereira, A.V., Fernandes, D., Manente, F.A., Vellosa, J.C.R., Nepel, A., Barison, A., Beltrame, F.L., 2014. Chemical and pharmacological investigation of the stem bark of *Synadenium grantii* Hook. f. Planta Med. 80, 458–464.

Nađpal, J.D., Lesjak, M.M., Šibul, F.S., Anačkov, G.T., Četojević-Simin, D.D., Mimica-Dukić, N.M., Beara, I.N., 2016. Comparative study of biological activities and phytochemical composition of two rose hips and their preserves: *Rosa canina* L. and *Rosa arvensis* Huds. Food Chem. 192, 907–914.

Nascimento, G.G.F., Locatelli, J., Freitas, P.C., Silva, G.L., 2000. Antibacterial activity of plant extracts and phytochemicals on antibiotic resistant bacteria. Braz. J. Microbiol. 31, 247–256.

Pellegrini, N., Re, R., Yang, M., Evans, C.R., 1998. Screening of dietary carotenoids and carotenoid-rich fruit extracts for antioxidant activities applying 2,2′-azinobis(3-ethylenebenzothiazoline-6 sulfonic acid) radical cation decolorization assay. Methods Enzymol. 299, 379–389.

Peniche, C., Zaldívar, D., Bulay, A., Román, J.S., 1992. Study of the thermal degradation of poly(furfuryl methacylato) by thermogravimetry. Polym. Degrad. Stab. 40, 287–295.

Pfaller, M.A., Boyken, L., Messer, S.A., Hollis, R.J., Diekema, D.J., 2004. Stability of Mueller-Hinton agar supplemented with glucose and methylene blue for disk diffusion testing of fluconazole and voriconazole. J. Clin. Microbiol. 42, 1288–1289.

Prashanth, K.V.H., Kittur, F.S., Tharanathan, R.N., 2002. Solid state structure of chitosan prepared under different N-deacetylating conditions. Carbohydr. Polym. 50, 27–33.

Prichystalová, H., Almonasy, N., Abdel-Mohsen, A.M., Abdel-Rahman, R.M., Vojtova, L., Kobera, L., Spotz, Z., Burgert, L., Jancar, J., 2014. Synthesis, characterization and antibacterial activity of new fluorescent chitosan derivatives. Int. J. Biol. Macromol. 65, 234–240.

Quideau, S., Deffieux, D., Douat-Casassus, C., Pouységu, L., 2011. Plant polyphenols: chemical properties, biological activities and synthesis. Angew. Chem. Int. Ed. 50, 586–621.

Ramos-Tejada, M.M., Durán, J.D.G., Ontiveros-Ortega, A., Espinosa-Jimenez, M., Perea-Carpio, R., Chibowski, E., 2002. Investigation of alumina/(+)-catechin system properties, Part I: a study of the system by FTIR-UV–vis spectroscopy. Colloid Surf. B 24, 297–308.

Rubilar, J.F., Cruz, R.M.S., Silva, H.D., Vicente, A.A., Khmelinskii, I., Vieira, M.C., 2013. Physico-mechanical properties of chitosan films with carvacrol and grape seed extract. J. Food Eng. 115, 466–474.

Senel, S., Mcclure, S.J., 2004. Potential applications of chitosan in veterinary medicine. Adv. Drug Deliv. Rev. 56, 1467–1480.

Silva, L.C., Pegoraro, K.A., Pereira, A.V., Esmerino, L.A., Cass, Q.B., Barison, A., Beltrame, F.L., 2011. Antimicrobial activity of *Alternanthera brasiliana* Kuntze (Amaranthaceae): a biomonitored study. Lat. Am. J. Pharm. 30, 147–153.

Siripatrawan, U., Harte, B.R., 2010. Physical properties and antioxidant activity of an active film from chitosan incorporated with green tea extract. Food Hydrocolloid. 24, 770–775.

Soares, J.R., Dinis, T.C., Cunha, A.P., Almeida, L.M., 1997. Antioxidant activities of some extracts of *Thymuszygis*. Free Radic. Res. 26, 469–478.

Song, Y., Jeong, S.W., Lee, W.S., Park, S., Kim, Y.-H., Kim, G.-S., Lee, S.J., Jin, J.S., Kim, C.-Y., Lee, J.E., Ok, S.Y., Bark, K.-M., Shin, S.C., 2014. Determination of polyphenol components of Korean prostrate spurge (*Euphorbia supina*) by using liquid chromatography-tandem mass spectrometry: overall contribution to antioxidant activity. J. Anal. Methods Chem. 1, 1–8.

Timmers, M.A., Guerrero-Medina, J.L., Esposito, D., Grace, M.H., Paredes-Lopez, O., García-Saucedo, P.A., Lila, M.A., 2015. Characterization of phenolic compounds and antioxidant and antiinflammatory activities from mamuyo (*Styrax ramirezii* Greenm.) fruit. J. Agric. Food Chem. 63, 10459–10465.

Torreggiani, A., Jurasekova, Z., Sanchez-Cortes, S., Tamba, M., 2008. Spectroscopic and pulse radiolysis studies of the antioxidant properties of (+)catechin: metal chelation and oxidizing radical scavenging. J. Raman Spectrosc. 39, 265–275.

Tripathi, S., Mehrotra, G.K., Dutta, P.K., 2008. Chitosan based antimicrobial films for food packaging applications. E-Polymers 93, 1–7.

Vieira, R.S., Beppu, M.M., 2006. Interaction of natural and cross linked chitosan membranes with Hg(II)ions. Colloids Surf. A 279, 196–207.

Wang, L., Dong, Y., Men, H., Tong, J., Zhou, J., 2013. Preparation and characterization of active films based on chitosan incorporated tea polyphenols. Food Hydrocolloid. 32, 35–41.

Zhang, H., Zhao, Y., 2015. Preparation, characterization and evaluation of tea polyphenole-Zn complex loaded β-chitosan nanoparticles. Food Hydrocolloid. 48, 260–273.

Zhang, L., Kosaraju, S.L., 2007. Biopolymeric delivery system for controlled release of polyphenolic antioxidants. Eur. Polym. J. 43, 2956–2966.

Zhang, C., Ding, Y., Ping, Q., Yu, L.L., 2006. Novel chitosan-derived nanomaterials and their micelle-forming properties. J. Agric. Food Chem. 54, 8409–8416.